We are IntechOpen, the world's leading publisher of Open Access books Built by scientists, for scientists

4,200
Open access books available

116,000
International authors and editors

125M
Downloads

Our authors are among the

154
Countries delivered to

TOP 1%
most cited scientists

12.2%
Contributors from top 500 universities

BOOK CITATION INDEX
CLARIVATE ANALYTICS
INDEXED

WEB OF SCIENCE™

Selection of our books indexed in the Book Citation Index
in Web of Science™ Core Collection (BKCI)

Interested in publishing with us?
Contact book.department@intechopen.com

Numbers displayed above are based on latest data collected.
For more information visit www.intechopen.com

Experimental Research on Development Energy Efficiency of Non-Thermal Plasma Technology

Tao Zhu

Additional information is available at the end of the chapter

http://dx.doi.org/10.5772/58881

1. Introduction

NTP has been recently used to distinguish the one-atmosphere, near room temperature plasma discharges from other plasmas, operating at hundreds or thousands of degrees above ambient. Industrially applied plasma technologies, is that they are 1) non-thermal and 2) operate at or near atmospheric pressure. NTP is a new technology for environmental protection, especially in the field of air pollution control, and has been studied by many researchers for 20 years [1]. Due to NTP generated at normal temperature and atmospheric pressure, easy operation and higher treatment efficiency, compare to the other technologies [2]. So far, NTP technology has been used in many fields and decomposed many kinds of air pollutants. There are many researches focusing on volatile organic compounds (VOCs) decomposition [3], and SO_2 and NOx degradations [4,5], and CFCs and odors and mercury treatments [6-8], etc. But during of NTP technology development and application, there is a key problem restricting NTP technology for commercial application [9], that is, how to solve energy consumption [10,11].

In order to resolve this problem, a series of researches were carried out in the world. Platinum based catalyst with NTP generated by a high voltage bipolar pulsed excitation was adopted by some researchers [12]. They found the energy efficiency is 0.14 mol/kWh for 2-Heptanone decomposition when the energy density is 200 J/L, and the energy efficiency decreased to 0.029 mol/kWh using an uncoated monolith when the energy density is 500 J/L. Ogata *et al.* [13] used NTP reactor packed with $BaTiO_3$ pellets to decompose the aromatics benzene, toluene and *o*-xylene. The results show $BaTiO_3$ pellets have a function for enhancing electric field strength and improving VOCs decomposition.

In our research, we developed a new ferroelectric packed bed NTP reactor and prepared a sample of $Ba_{0.8}Sr_{0.2}Zr_{0.1}Ti_{0.9}O_3$. Doped some ions (Sr & Zr) into the powder particles and crystal boundary in the experiment, the metal ions such as strontium, zinc and zirconium entered into

crystal lattices of $BaTiO_3$ equably and the Curie temperature (Tc) fell [14]. Because of higher permittivity and lower dielectric loss of $Ba_{0.8}Sr_{0.2}Zr_{0.1}Ti_{0.9}O_3$ than those of $BaTiO_3$, $Ba_{0.8}Sr_{0.2}Zr_{0.1}Ti_{0.9}O_3$ shows a better ferroelectric physical property to increase the energy efficiency for VOCs removal.

2. Material and methods

2.1. NTP System

The NTP system consisted of a tube-wire packed-bed reactor system, an AC power supply, a continuous flow gas supplying system and an electric and gaseous analytical system [14]. Dry air (78% N_2, 21% O_2) was used as a balance gas for toluene decomposition. The whole NTP system refer to reference [14]. The NTP packed-bed reactor was shown in Fig.1. And the schematic diagram of NTP system is shown in Fig.2. As the packed materials in NTP reactors, we selected four packed materials, respectively, including no packed materials, ceramic rings, $BaTiO_3$ rings and $Ba_{0.8}Sr_{0.2}Zr_{0.1}Ti_{0.9}O_3$ rings [14].
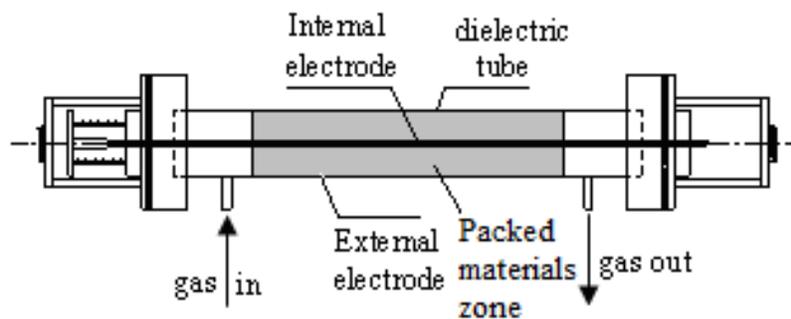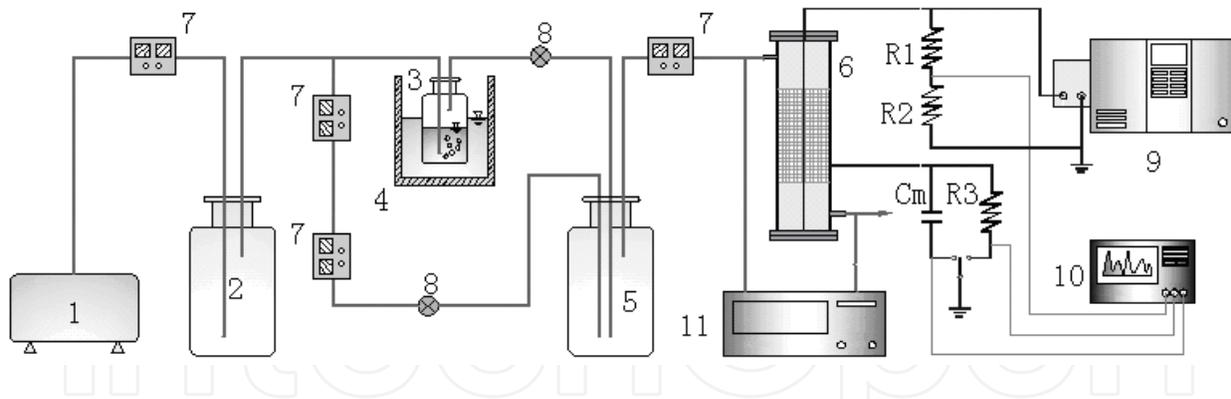

Figure 1. NTP reactor

Reactor: organic-glass tube (i.d.32mm, packed infilling length of packed materials of 200mm); Internal electrode: tungsten filament (i.d.0.5mm); External electrode: dense steel mesh; Packed materials packed in the dark zone, respectively selected ceramic rings, $BaTiO_3$ rings and $Ba_{0.8}Sr_{0.2}Zr_{0.1}Ti_{0.9}O_3$ rings. (after T.Zhu [14])

2.2. Materials and methods

In the experiment, three kinds of packed materials, including ceramic rings, $BaTiO_3$ rings and $Ba_{0.8}Sr_{0.2}Zr_{0.1}Ti_{0.9}O_3$ rings (hollow cylinder shape, 5 mm i.d., 1 mm wall thick, and 10 mm length), were used to pack into the NTP reactor.

We use the method of water-thermal composite action to prepare a kind of modified ferro-electric of nano-size $Ba_{0.8}Sr_{0.2}Zr_{0.1}Ti_{0.9}O_3$ powder at atmospheric pressure. The prepared detail of nano-$Ba_{0.8}Sr_{0.2}Zr_{0.1}Ti_{0.9}O_3$ refers to our former research [15].

Figure 2. Schematic diagram of NTP system for toluene removal 1.air compressor 2.buffer 3.toluene liquid bottle 4.at-temperator 5.blender 6.NTP reactor 7.mass flow meter 8.needle valve 9.high voltage 10. oscilloscopes 11.gas chromatograph

We detected the crystal structures and the surface conditions of the $Ba_{0.8}Sr_{0.2}Zr_{0.1}Ti_{0.9}O_3$ samples by XRD (manufactured by Germany Bruker Co., D8 ADVANCE) and SEM (manufactured by Japan, JEOL-JSM-6500F). We used Micromeritics (manufactured by American Quantachrome Co., NOVA 1000) to determine BET surface area. Using an LCR automatism test instrument (manufactured by China, 4210), we measured the relative permittivity of $Ba_{0.8}Sr_{0.2}Zr_{0.1}Ti_{0.9}O_3$ samples. Toluene analysis was carried out by gas chromatography (manufactured by Aglient Co., HP6890N) with a flame ionization detector (FID). The byproducts were detected by GC-MS (manufactured by American Thermo Finnegan Co.) using EI mode, 70 eV and full scan. Ozone concentration produced in the NTP reactor was measured by an iodine-titration method. The plasma reactor employed an AC power supply of 150 Hz scanning from 0 kV to 100 kV was applied to the reactor in the radial direction. The voltage and current waveforms were measured by oscillograph (manufactured by American Tektronix Co., TDS2014). To investigate the electric characteristics of dielectric barrier discharge (DBD), the voltage applied to the reactor was sampled by a voltage divider with a ratio of 12500:1. Also, the current was determined from the voltage drop across a shunt resistor (R3 =10kΩ) connected in series with the grounded electrode. In order to obtained the total charge and discharge power simulta-neously, a capacitor (Cm =2μF) was inserted between the reactor and the ground. The electrical power provided to the discharge was measured using the Q–V Lissajous diagram. Typical Lissajous diagram represents to be a parallelogram, and we could calculate power though calculated the area of parallelogram. The whole methods can be seen in the reference [14].

The removal efficiency, reactor energy density, and energy efficiency of toluene were calcu-lated in the process of NTP as follows [14]:

Toluene removal efficiency (η):

$$\eta(\%) = \frac{[toluene]_{inlet} - [toluene]_{outlet}}{[toluene]_{inlet}} \times 100\% \tag{1}$$

Reactor Input energy density (RED):

$$RED(kJ / L) = \frac{input \cdot power(W)}{gas \cdot flow \cdot rate(L / \min)} \times 60 \times 10^{-3} \tag{2}$$

Energy efficiency (ζ):

$$\zeta(g / kWh) = \frac{[toluene]_{inlet} \times \eta}{RED} \times 3.6 \times 10^{-3} \tag{3}$$

3. Results and discussion

3.1. Detection of modified ferroelectric

The crystal structure of $Ba_{0.8}Sr_{0.2}Zr_{0.1}Ti_{0.9}O_3$ is detected by XRD as shown in Fig.3. From Fig.3, we can think the crystal structure of $Ba_{0.8}Sr_{0.2}Zr_{0.1}Ti_{0.9}O_3$ is a kind of ferroelectric, and very close to $BaTiO_3$ and 59 nm diameter. That means crystal structure of nano-$Ba_{0.8}Sr_{0.2}Zr_{0.1}Ti_{0.9}O_3$ should be a kind of cube crystal structure of calcium-titanium oxide. The BET surface area of $Ba_{0.8}Sr_{0.2}Zr_{0.1}Ti_{0.9}O_3$ are 8.8 m^2/g, and Longmuir surface area is 12.3 m^2/g or so. The relative permittivity of $Ba_{0.8}Sr_{0.2} Zr_{0.1}Ti_{0.9}O_3$ is 12000.
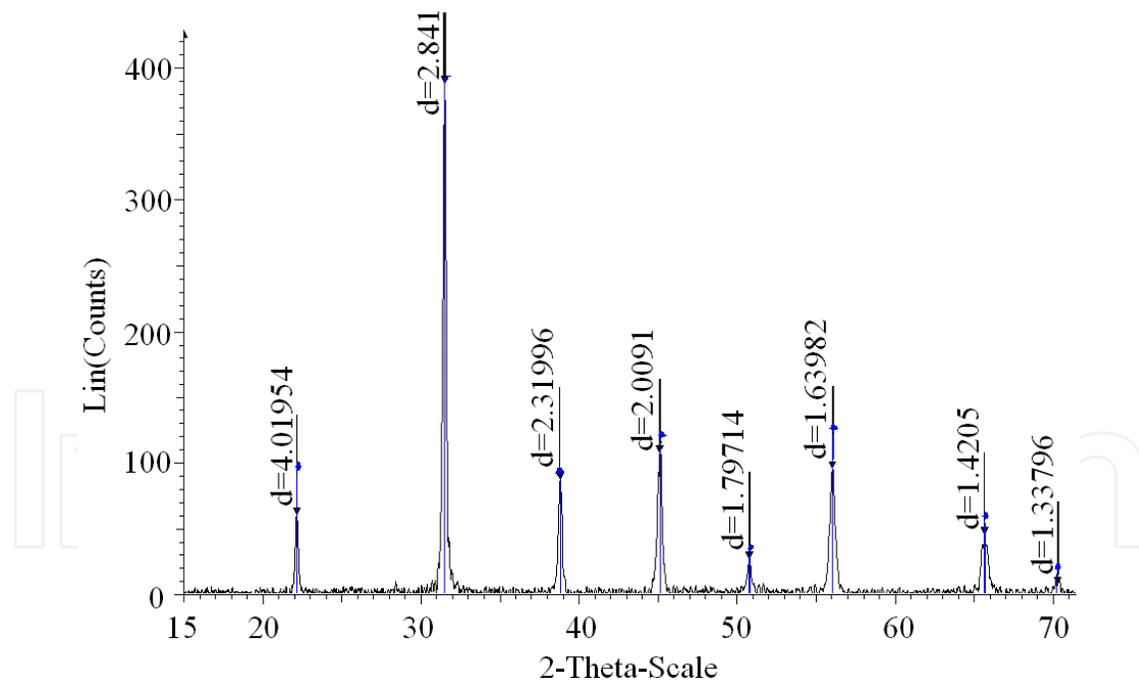

Figure 3. XRD testing results of $Ba_{0.8}Sr_{0.2}Zr_{0.1}Ti_{0.9}O_3$

3.2. Effect of nano-$Ba_{0.8}Sr_{0.2}Zr_{0.1}Ti_{0.9}O_3$ on toluene decomposition

Fig.4 shows the effect of nano-$Ba_{0.8}Sr_{0.2}Zr_{0.1}Ti_{0.9}O_3$ on toluene removal efficiency (toluene: 600 mg/m^3; flow velocity: 1 mL/min; dry air) [14]. At the same RED, the removal efficien-

cy of toluene had an order of no packed materials < ceramic rings < $BaTiO_3$ rings < nano-$Ba_{0.8}Sr_{0.2}Zr_{0.1}Ti_{0.9}O_3$ rings. Packed materials in NTP reactor could effectively enhance the energy intensity of input reactor and accelerated toluene decomposition. NTP operating at the RED of 0.76 kJ/L, toluene removal efficiency arrived at 97% and the energy efficiency attained 6.48 g/kWh when the packed materials of $Ba_{0.8}Sr_{0.2}Zr_{0.1}Ti_{0.9}O_3$ are used in NTP reactor [14].

In the electrode gap, if we add the presence of solid material, NTP will be enhance, and homogeneous plasma would be formed rather than a filamentous one. Eliasson et al. [16] found that it is important to pack the packed materials into NTP reactor, and the more high energy electrons properly generated by dielectric barrier discharge (DBD). Due to high energy electrons could destroy the molecular structure of toluene, the removal efficiency is increasing with the numbers of high energy electrons increase.

During the preparation of $Ba_{0.8}Sr_{0.2}Zr_{0.1}Ti_{0.9}O_3$ samples, strontium (Sr) and zirconium (Zr) metal ions can enter crystal lattices of $BaTiO_3$ equably and lower the Curie temperature (Tc) [17]. As a result, the permittivity of $Ba_{0.8}Sr_{0.2}Zr_{0.1}Ti_{0.9}O_3$ is 12000, 8 times higher than that of pure phase of $BaTiO_3$ (1500) in room temperature [15]. According to Yamamoto et al.[18], the permittivity had a significant influence on the discharge energy of NTP reactor.
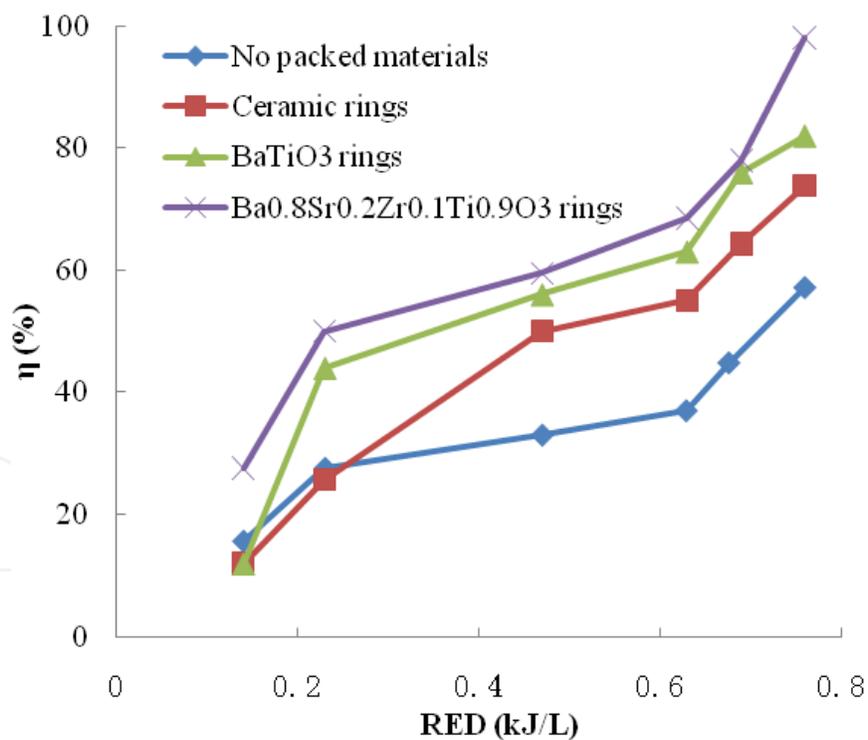

Figure 4. Relationship between RED and removal efficiency in four NTP reactors

Fig.5 shows the ozone (O_3) concentration with and without the packed materials [14]. O_3 concentration is the highest with $Ba_{0.8}Sr_{0.2}Zr_{0.1}Ti_{0.9}O_3$ and is in the order of no packed materials < ceramic rings <$BaTiO_3$ rings < $Ba_{0.8}Sr_{0.2}Zr_{0.1}Ti_{0.9}O_3$ rings at the identical RED.

As a kind of main long-living radicals, O_3 was generated and transported to the packed materials to take part in oxidation reaction on the surface of packed materials [14, 19].

$$e + O_2 \rightarrow 2O + e \tag{4}$$

$$O + O_2 + M \rightarrow O_3 + M \tag{5}$$

$$O + O_3 \rightarrow 2O_2 \tag{6}$$

$$e + O_3 \rightarrow O + O_2 + e \tag{7}$$

In fig.6, we can find O_3 concentration increases when REDs change from 0 to 0.7 kJ/L, and the maximum ozone concentration appears at the RED of 7 kJ/L. Yamamoto et al. also found the same change of the pattern of ozone production [20]. $Ba_{0.8}Sr_{0.2}Zr_{0.1}Ti_{0.9}O_3$ has higher relative permittivity than $BaTiO_3$ so that $Ba_{0.8}Sr_{0.2}Zr_{0.1}Ti_{0.9}O_3$ can be electric polarized at normal temperature. Therefore, electric field strength and RED are enhanced significantly [14]. As a result, O_3 concentration increases according to Eq.(6) (RED ≤ 0.7 kJ/L). While RED ≥ 0.7 kJ/L, the superfluous high-energy electrons accelerate O_3 to transform into O_2 according to Eq.(7) and Eq.(8).
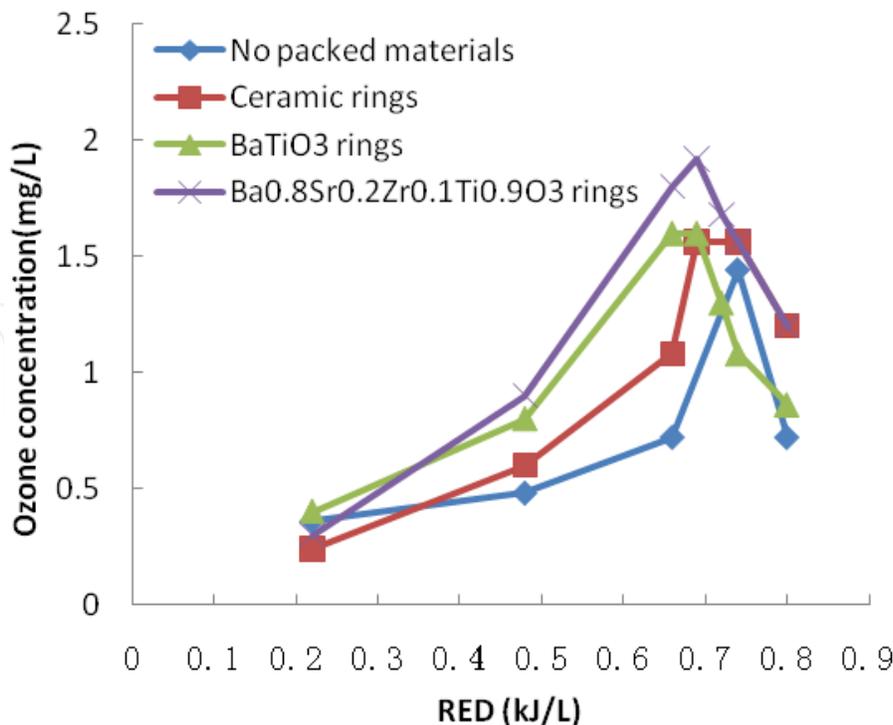

Figure 5. Relationship between RED and ozone concentration in four NTP reactors

Chang et al.[21] found that there are two main mechanisms for VOC decomposition. 1) Directly, electrons attack VOC molecules. 2) indirectly reactions happen between VOC molecules and radicals. And these radicals involve oxygen plasma, free radical groups, ozone, etc. Chang's results indicate higher O_3 concentration is positive to higher removal efficiency. So as packed materials, $Ba_{0.8}Sr_{0.2}Zr_{0.1}Ti_{0.9}O_3$ seems to be better than $BaTiO_3$.

Fig.6 shows the change of energy efficiency (ζ) for toluene removal under the different conditions [14]. The energy efficiency has an order as show as follows at the same RED: no packed materials <ceramic rings <$BaTiO_3$ rings < $Ba_{0.8}Sr_{0.2}Zr_{0.1}Ti_{0.9}O_3$ rings. The energy efficiency is 15 g/kWh with $Ba_{0.8}Sr_{0.2}Zr_{0.1}Ti_{0.9}O_3$ and 11 g/kWh with $BaTiO_3$ at RED of 0.23 kJ/L in the NTP reactor. The results show that $Ba_{0.8}Sr_{0.2}Zr_{0.1}Ti_{0.9}O_3$ has a better ferroelectric property to improve energy efficiency and reduce energy consumption in the NTP process for VOCs control, compared with $BaTiO_3$.

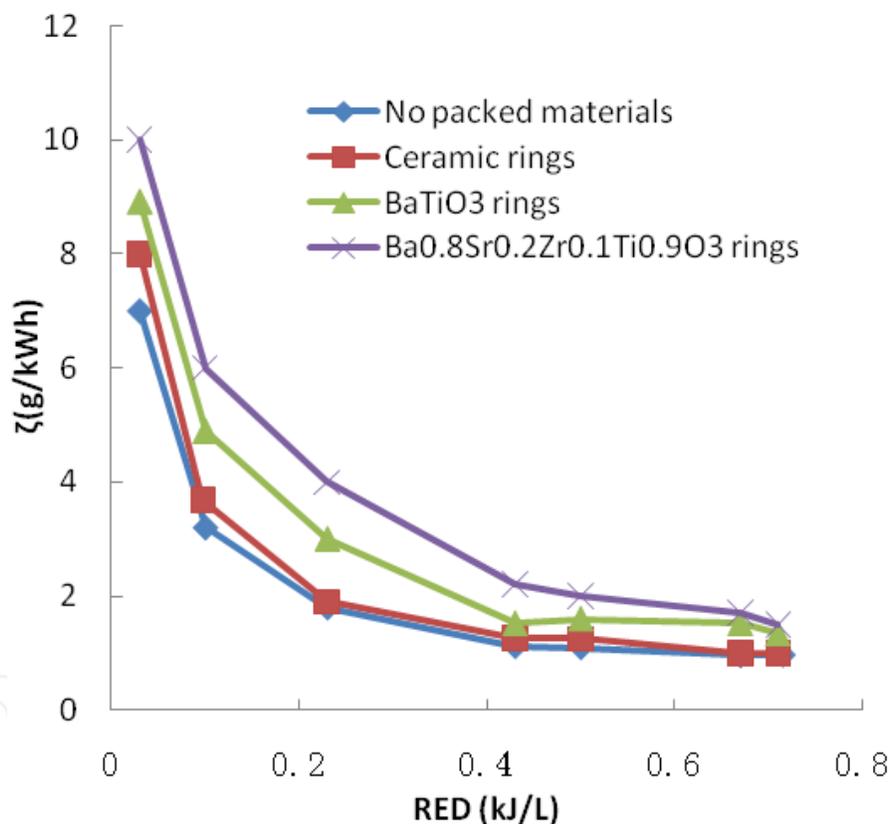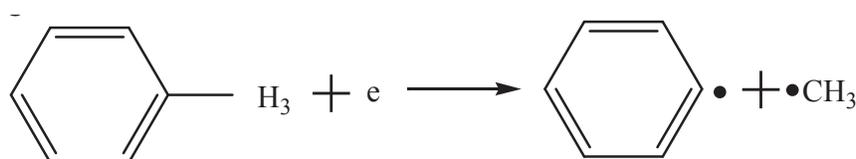**Figure 6.** Relationship between RED and energy efficiency in four NTP reactors

3.3. Byproducts analysis

In the process of toluene abatement, the emission in the outlet was detected by GC-MS at electric field strength of 8 kV/cm in Fig.7 (a). By NIST2000 mass spectrum, the polymerization products formation can be observed, including aldehyde, alcohols, amide, and benzene derivative [22].

In fig.7 (b), the byproducts are very few at electric field strength of 14 kV/cm. We can assume that toluene molecules would be completely oxidized to CO_2, CO and H_2O in the enough high electric field strength of the enough high input power. In fact, there are a large number of high-energy electrons, ions and free radicals in NTP process. Firstly, eq.(5~8) indicate high-energy electrons take part in reaction with oxygen in air [22]. And at the same time, high-energy electron reacted with H_2O and N_2 in contaminated air:

$$e + O_2 \rightarrow 2O^\bullet \tag{8}$$

$$e + H_2O \rightarrow 2H^\bullet + O^\bullet \tag{9}$$

$$e + H_2O \rightarrow OH^\bullet + H^\bullet + e \tag{10}$$

$$e + 2H_2O \rightarrow HO_2^\bullet + 3H^\bullet + e \tag{11}$$

$$e + N_2 \rightarrow 2N^\bullet + e \tag{12}$$

Toluene bond energy between carbon of benzene ring and carbon of substituent radical is 3.6 eV, which is the lowest than that of carbon-carbon bond or hydrocarbon bond. Hydrogen of benzene ring is replaced by methyl, which lead to the stability of benzene ring is broken [14]. So molecule structure of toluene is not stable. In the theoretical point of view, this bond is the most vulnerable and broken. Of course, the other bonds are also likely to be destroyed by high energy electrons. Eq.13 is the possible reaction equations of the process of toluene decomposition [23].
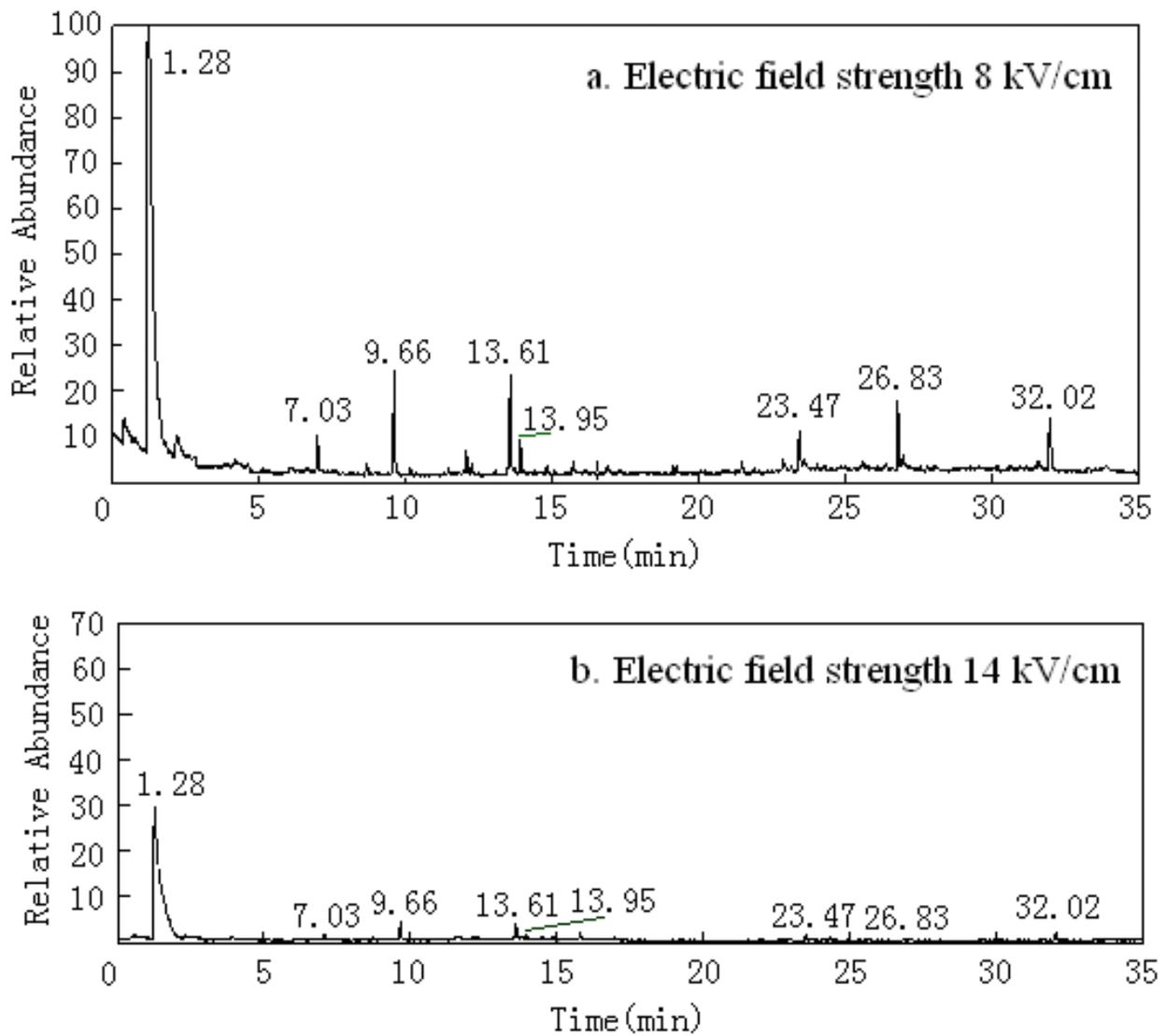
$$\text{(benzene ring)}-H_3 + e \longrightarrow \text{(benzene ring)}-CH_3 + \bullet H$$

$$C\text{(benzene ring)}-H_3 + e \longrightarrow H\overset{\bullet}{C}=CH-C=\overset{\bullet}{C}H + H\overset{\bullet}{C}=\overset{\bullet}{C}-CH_3$$

$$\text{(benzene ring)}-H_3 + e \longrightarrow H\overset{\bullet}{C}=\overset{\bullet}{C}H + H\overset{\bullet}{C}=CH-C=\overset{\bullet}{C}H \quad (CH_3)$$

$$\text{(benzene ring)}-H_3 + e \xrightarrow{\geq 5.5eV} \overset{\bullet}{C}H_2-\underset{H}{C}=\underset{H}{C}-\underset{H}{C}=\underset{H}{C}-\overset{\bullet}{C}H_2$$

Aldehyde, alcohols, amide, and benzene derivative were form in NTP process during above all of free radical groups reacted with the other reaction fragments. When energy efficiency continuing to increase, the byproducts ought to degraded into CO_2, CO and H_2O.

Figure 7. Mass spectrum of byproducts of toluene decomposition

4. Conclusion

In this paper, NTP was generated by DBD at 20℃ and 1 atm. We selected four kinds of packed materials, including no padding, ceramic rings, $BaTiO_3$ rings and $Ba_{0.8}Sr_{0.2}Zr_{0.1}Ti_{0.9}O_3$ rings, which to pack into NTP reactor. Nano-$Ba_{0.8}Sr_{0.2}Zr_{0.1}Ti_{0.9}O_3$ was prepared by the method of water-thermal composite action in our laboratory. By detected, $Ba_{0.8}Sr_{0.2}Zr_{0.1}Ti_{0.9}O_3$ shows better ferroelectric characteristic than $BaTiO_3$. Then this kind of new modified ferroelectric of $Ba_{0.8}Sr_{0.2}Zr_{0.1}Ti_{0.9}O_3$ as the packed materials is used in the packed bed NTP reactor for the first time. During the whole experiments, we attained the best removal efficiency of toluene and the best energy efficiency with $Ba_{0.8}Sr_{0.2}Zr_{0.1}Ti_{0.9}O_3$ rings as packed materials in NTP reactor. For example, toluene removal efficiency arrived at 97% and the energy efficiency stopped at

6.48 g/kWh when RED was 0.76 kJ/L or so, and ozone concentration reached the maximum value when RED was 0.7 kJ/L or so. Ozone concentration is positive to higher removal efficiency. There are aldehyde, alcohols, amide, and benzene derivative, which generated as the byproducts in NTP process and detected by GC-MS. Of course, these byproducts could be decomposed into CO_2, CO and H_2O entirely at last if we further increased input energy intensity. So nano-$Ba_{0.8}Sr_{0.2}Zr_{0.1}Ti_{0.9}O_3$ as the packed materials in the packed bed NTP reactor would effectively improve energy efficiency for VOCs removal than the other packed materials in NTP reactor.

Acknowledgements

Author details

Tao Zhu[*]

Address all correspondence to: bamboozt@cumtb.edu.cn

School Chemical & Environmental Engineering, China University of Mining & Technology-Beijing, Beijing, China

References

[1] S. Masuda, S. Hosokawa, and X. L Tu. The performance of an integrated air purifier for control of aerosol, microbial, and odor. *IEEE Trans. Ind. Appl*. 29, 774-780, 1993.

[2] B. Eliasson, and U. Kogelschatz. Nonequilibrium volume plasma chemical processing. *IEEE Trans. Plasma Sci*. 1991, 19, 1063-1068.

[3] T. Zhu, J. Li, Y. Q. Jin, and G. D. Ma. Gaseous phase benzene decomposition by non-thermal plasma coupled with nano-titania catalyst. *Int. J. Environ. Sci. Tech.* 2008, 6 (1), 141-148.

[4] M. B. Chang, J. H. Balbach, M. J. Rood, and M. J. Kushner. Removal of SO_2 from gas streams using a dielectric barrier discharge and combined plasma photolysis. *J. Appl. Phys*. 1991, 69, 4409-4418.

[5] Y.S. Mok, M. Dors, J. Mizeraczyk. Effect of reaction temperature on NOx removal and formation of ammonium nitrate in nonthermal plasma process combined with selective catalytic reduction. *IEEE Trans. Plasma Sci.* 2004, 32, 799-807.

[6] C. L. Ricketts, A. E. Wallis, and J. C. Whitehead. A mechanism for the destruction of CFC-12 in a nonthermal, atmospheric pressure plasma. *J. Phys. Chem. A*. 2004, 108, 8341-8345.

[7] M. B. Chang, and T. D. Tseng. Gas-phase removal of H_2S and NH_3 with dielectric barrier discharges. *J. Environ. Eng.* 1996, 122, 41-46.

[8] S. Masuda, Pulse corona induced plasma chemical process: a horizon of new plasma chemical technologies. *Pure Appl. Chem.* 1988, 60, 727-731.

[9] T.Zhu, J.Li, Y.Q.Jin, et al. Research Progresses in Treatment of Waste Gas Containing Volatile Organic Compounds by Combined Plasma Technology. *Environ. Protec. Chem. Ind.* 2008, 28 (2), 121-125.

[10] J. Van Durme, J. Dewulf, C. Leys, H. Langenhove: Combining non-thermal plasma with heterogeneous catalysis in waste gas treatment: A review, *Appl. Cata. B: Environ*. 2008, 78, 324-333.

[11] T. Zhu, J. Li, W. J. Liang, Y. Q. Jin. Synergistic effect of catalyst for oxidation removal of toluene. J. Hazard. Mater. 2009, 165,1258-1260.

[12] C. Ayrault, J. Barrault, N. Blin-Simiand, F. Jorand, S. Pasquiers, A. Rousseau, J. M. Tatibouet. Oxidation of 2-heptanone in air by a DBD type plasma generated within a honeycomb monolith supported Pt-based catalyst, Cata. Today. 2003, 89, 75-83.

[13] A.Ogata, H.Einaga, H.Kabashima, et al. Effective combination of nonthermal plasma and catalysts for decomposition of benzene in air. *Appl. Catal. B: Environ.* 2003, 46(1), 87-95.

[14] Tao Zhu, Yandong Wan, Hairong Li, Che Sha, Yan Fang. VOCs decomposition via modified ferroelectric packed bed dielectric barrier discharge plasma, *IEEE Trans. Plasma Sci.*, 2011, 39(8), 1695-1700.

[15] Tao Zhu. Chemistry, emission control, radioactive pollution and indoor air quality, Chapter 4. InTech Publisher, 2011.

[16] B. Eliasson, U. Kogelschatz. Nonequilibrium volume plasma chemical processing, *IEEE Trans. Plasma Sci*. 1991, 19, 1063-1068.

[17] S. W. Ding, J. Wang, J. L. Qin. The structure and performance of complex of nanometer $BaTiO_3$, *Sci. China, Ser. B*. 2001, 31, 525-529.

[18] T. Yamamoto, K. Ramanatiran, P. A. Lawless, D. S. Ensor, J. R. Nwesome, N. Plaks, G. H. Ramsey. Control of Volatile organic compound by ac energized ferroelectric pellet reactor and a pulsed corona reactor, IEEE Trans. Ind. Appl. 1992, 28, 528-532.

[19] S. Delagrange, L. Pinard, J. M. Tatiboue°t. Combination of a non-thermal plasma and a catalyst for toluene removal from air: Manganese based oxide catalysts, Appl. Cat-al. B: Environ. 2007, 68, 92-98.

[20] T. Yamamoto. Methods and apparatus for controlling toxic compounds using cataly-sis-assisted non-thermal plasma, Environ. Int. 1997, 23, 3-10.

[21] M. B. Chang, C. C. Lee. Destruction of formaldehyde with dielectric barrier discharge plasmas, Environ. Sci. Tech. 1995, 29, 181-186.

[22] Tao Zhu. Toluene removal using non-thermal plasma technology coupled with nano-$Ba_{0.8}Sr_{0.2}Zr_{0.1}Ti_{0.9}O_3$. 2010 4th International Conference on Bioinformatics and Biomedi-cal Engineering, 06/2010.

[23] Atkinson R., Pitts J.N., Jr. Kinetics and mechanism of the gas phase reaction of hy-droxyl radicals with aromatic hydrocarbons over the temperature range 296-473 K. J. Phys. Chem. 1977, 81(4), 296–304.